Tunnelling and Underground Space Technology 81 (2018) 1–15

Contents lists available at ScienceDirect

Tunnelling and Underground Space Technology

journal homepage: www.elsevier.com/locate/tust

Failure characteristics and stress distribution of pre-stressed rock specimen with circular cavity subjected to dynamic loading

Ming Tao[a], Huatao Zhao[a], Xibing Li[a], Xiang Li[a], Kun Du[b,*]

[a] School of Resources and Safety Engineering, Central South University, Changsha, Hunan, China
[b] Advanced Research Center, Central South University, Changsha, Hunan, China

ARTICLE INFO

Keywords:
Static pre-stress
Dynamic loading
Cavity
Violent ejection

ABSTRACT

A modified Hopkinson pressure bar system with coupled static and dynamic disturbance is used to study the failure characteristics of a granite specimen with a cavity. Different coupled static pre-stress and dynamic loading experiments are conducted. The dynamic failure processes and characteristics of the granite specimen with a cavity under the test conditions are summarised. High speed camera images showed that moderate static pre-stresses of 27 MPa and 36 MPa coupled with moderate dynamic loading of 168 MPa lead to violent rock failure, which is the same as rock-burst. In addition, the coupled static pre-stress and dynamic loading processes are simulated, and the dynamic stress concentration factors (DSCFs) and strain energy density (SED) around the cavity under different coupled loads are investigated. The simulation results show that violent rock failure occurs at a higher DSCF and SED. The experimental and numerical setup used in this study provides useful results for investigating the characteristics of rock failure under coupled static and dynamic stress conditions.

1. Introduction

Studies on the influence of cavities on the strength and other failure characteristics of rock have been ongoing for many years. The problem and its solutions involve two different areas of concern: brittle fracture mechanics on a microscopic scale, which are considered stress raisers, and mining and tunnelling operations. Under increasing uniaxial compressive stress, Carter et al. (1991) demonstrated that the failure patterns of rock specimens containing a circular cavity will typically undergo evolutionary processes: primary tensile fracture, secondary or remote fracture, and sidewall slabbing or compressional failure. Hoek and Brown (1980) related the remote fracturing to the tensile stress concentrations that form remotely from the opening. Lajtai et al. (1991), Lajtai and Lajtai (1975) reported that the remote fractures combined ultimately with the failure process in the compression zone causing the collapse of the cavity. Carter (1992) reported on the effect of hole size on fracture initiation around cavities in a rock with studies involving physical models of Tyndall limestone. Zhao et al. (2014) reported that granite blocks containing one pre-existing cylindrical cavity under uniaxial compression can be characterised by tensile cracking on the roof and floor. More recently, acoustic emissions have been used to study the evolution of cavity breakouts. For example, Aker et al. (2014) studied the acoustic emissions associated with shear and tensile failures around a horizontal borehole in a sandstone sample subjected to triaxial stress, which indicated that the anisotropic stress field influenced the macroscopic velocities and the resulting moment tensors.

In terms of numerical simulations, Zhu and Bruhns (2008); Zhu et al. (2014) simulated the failure process surrounding a circular hole using a finite element code, and the failure forms and maximum shear stress distributions were presented. Tomac and Gutierrez (2016) simulated the fracture propagation process around a cavity under axial compression using a discrete element code. Fakhimi et al. (2002) monitored the forces and displacements in a sandstone specimen with a circular cavity under biaxial compression. In addition, a number of theoretical models of borehole stability and failure analysis have been proposed (Hocking, 1976; Shao et al., 1994).

The above-mentioned studies reported primarily on the fracture evolution of rocks with circular holes under static compression. However, dynamic loading has a significant influence on rock failure characteristics, especially on defective rocks (Diederichs, 2007; Kaiser et al., 2001; Li et al., 2014; Wang et al., 2017a; Zhang and Zhao, 2014). Therefore, the dynamic properties of intact rock, including the stress-strain curves and failure modes, have been widely investigated using the split Hopkinson pressure bar (SHPB) technique (Xia et al., 2008; Xia et al., 2013; Zhou et al., 2010). Additionally, in deep excavations in hard rock mining subject to dynamic disturbance, a dynamic load is applied to rock in a static pre-stressed state, which leads to a coupled static and dynamic stress state. Kaiser (2012)) reported that rock failure

* Corresponding author at: Advanced Research Center, Central South University, Changsha, Hunan, 410083, China.
E-mail address: dukuncsu@csu.edu.cn (K. Du).

https://doi.org/10.1016/j.tust.2018.06.028
Received 30 October 2017; Received in revised form 26 March 2018; Accepted 27 June 2018

can be triggered by both remote seismic events and self-initiation. Wang et al. (2017b) reported that the damage to brittle materials can be caused by the accumulation of energy at the end of defects. Using a modified SHPB apparatus, Li et al. (2016), Li et al. (2008), Li et al. (2005) observed that rock failure mode and stress-strain relationships for coupled static and dynamic loads were different for rocks subjected to either a static stress or dynamic loading (Li et al., 2009; Tao et al., 2016; Weng et al., 2017). However, pre-stressed rocks with cavities subjected to dynamic loading have not been extensively studied. In fact, because of the cavities, the magnitude of the stress-field tensor changes, which can significantly influence the stability and strength characteristics. Therefore, it could be critical to record the coupled failure characteristics of pre-stressed rock with cavities subjected to dynamic loading.

In this study, a modified SHPB is used to investigate the processes associated with rock failure under coupled static and dynamic loading. Test under different uniaxial static pre-stresses, coupled with minor, moderate, and major dynamic loadings, are conducted on granite specimens containing holes. The rock failure process and rock debris ejections are discussed, based on high-speed camera images. In addition, the finite element programme LS-DYNA is used to simulate the loading process of rock under coupled static and dynamic loading, and the static and dynamic stress distributions are demonstrated. Finally, the dynamic damage characteristics of a deep tunnel in the Kaiyang Phosphorus Mine was studied. The results provided experimental and numerical data supporting the observation of different failure modes of a rock mass surrounding a cylindrical cavity under uniaxial coupled static and dynamic stress states.

2. Problem layout and experimental procedure

The static elasticity problem of a pre-stressed hole in a plate is well described by the Kirsch equation, which calculates stress concentrations in the vicinity of the hole. When pre-stressed rock with a hole is subjected to a dynamic disturbance, the energy of the dynamic disturbance is transmitted in the form of waves travelling through the rock and transmitted through the hole. The wave is reflected and scattered, giving rise to elevated local stress states such that dynamic stress concentrations are induced, as shown in Fig. 1.

When the superimposed static and dynamic stress concentrations exceed the strength of rock, rock failure will occur. Under a coupled static and dynamic stress state, in addition to conventional failures, rock could experience different failures from either static stress fields or dynamic loading. In order to obtain the characteristics of rock failure under these conditions, a coupled static-dynamic test platform, with a 50-mm-diameter modified SHPB was used in this study. The modified SHPB as shown in Fig. 2, was developed at the Central South University (Li et al., 2008), and can apply a static pre-stress, including axial and confining stress, before dynamic loading. The geometry and material properties of the modified SHPB have been reported in previous studies (Li et al., 2008). The elastic bars are of steel with a density of 7800 kg/m^3 and an elastic modulus of 240 GPa (Li et al., 2013). The rock

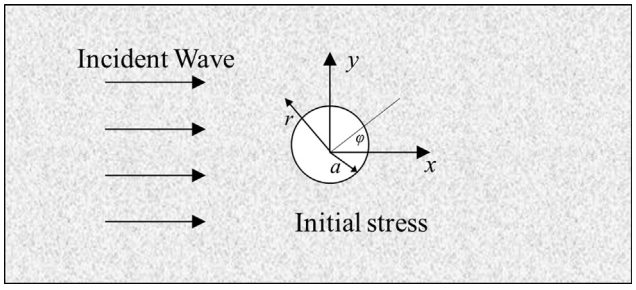

Fig. 1. Schematic diagram of pre-stressed rock with a circular cavity subject to dynamic disturbance.

specimens in the test were selected from a quarry in Miluo, Hunan, China, and have good homogeneity. The rock specimens were prepared with diameters of approximately 50 mm and aspect ratios of 2:1 (100 × 50 mm). An 8 mm-diameter hole was then drilled in the centre of the lateral surfaces, parallel to both the ends. Both ends and the lateral surfaces were carefully polished. The surface perpendicularity and roughness of the specimens were less than 0.01 mm and 0.02 mm, respectively. The specimens were placed between the input and output bars. A uniaxial static pre-stress was applied by the pre-load unit through two elastic bars. The dynamic stress waves generated by the impact of a striker driven by high pressure gas, with gradually increasing half-sine wave generated by modifying the shape of the striker bar.

3. Failure characteristics of rock specimen with cylindrical cavity

3.1. Static mechanical properties

The conventional static load test was first performed using an Instron 1346 hydraulic servo-controlled machine. All specimens were cored from the same granite block and considered homogeneous, with the following properties: density 2678 kg/m^3, Poisson's ratio 0.18, Young's modulus 44.62 GPa, P-wave velocity 4082 m/s, and uni-axial compression strength 112 MPa. The failure patterns for the rock specimens with a circular cavity under static uniaxial compression were obtained for increasing uniaxial compression, as shown in Fig. 3.

In Fig. 3, the cracks generated in the vicinity of the cavity (approximately twice the hole diameter) are defined as the primary-field cracks, and the cracks further from the hole (greater than twice the hole diameter) are defined as the remote-field cracks. During static testing, primary-field failures initiate first, forming at or near the rock wall perimeter and propagating away from the hole. Remote-field failures then form and propagate both away from and towards the cavity sidewalls. The near field failures gradually join with the remote field failures and cause the ultimate collapse of the rock specimen. Fig. 3 shows a typical failure band that occurs along the diagonal of the specimen associated with specimen dilatancy and a tension and shear mixed-mode failure process. During the failure process, the rock specimens gradually fail, and debris ejection or violent failure occurs.

In addition, previous studies indicated that violent failure can be induced in pre-stressed rock by dynamic disturbances (Du et al., 2016; He et al., 2010; Tao et al., 2017). However, the influence of the dynamic disturbances and the initial stress levels on the rock failure were not fully explored. In this study, the rock specimens have a cavity, and there are a static and dynamic stress concentration in the vicinity of the cavity, which could lead to different rock failures under dynamic loading. The static and dynamic loading levels can be accurately set on the test platform. The following section will demonstrate the failure characteristics of a uniaxial pre-stressed rock specimen with a cavity subjected to a dynamic disturbance, and various static pre-stresses and dynamic loadings will be investigated.

3.2. Coupling static and dynamic failure characteristics

High-speed cameras are commonly used for material tests under dynamic loading, because of the image size and frame rates (Xing et al., 2017; Xing et al., 2018). In this study, the dynamic failure process and the failure evolution of the specimens were captured by a high-speed camera (FASTCAM SA 1.1). The resolution used in this study was 320 × 176 at 100,000 fps, which records an image every 10 μs. The camera is triggered by a transistor logic level signal generated on an oscilloscope synchronised with the incident signal. The loading time and images are correlated after removing the short trigger delay. The time when the incident wave triggers the strain gauge at the input bar is treated as the starting time, i.e., 0 μs. The distance from the strain gauge to the specimen interfaces and input bar is 1 m, the wave velocity in the